General implications of aluminium speciation-dependent kinetic dissolution rate law in water–rock modelling

Article *in* Chemical Geology · October 1998

DOI: 10.1016/S0009-2541(98)00083-7

CITATIONS
21

READS
50

4 authors, including:

Frédéric Gérard
French National Institute for Agriculture, Food, and Enviro…
86 PUBLICATIONS **1,853** CITATIONS
SEE PROFILE

A. Clement
University of Strasbourg
54 PUBLICATIONS **802** CITATIONS
SEE PROFILE

Jean Louis Crovisier
University of Strasbourg
98 PUBLICATIONS **1,798** CITATIONS
SEE PROFILE

ELSEVIER

Journal of Contaminant Hydrology 30 (1998) 201–216

JOURNAL OF
Contaminant
Hydrology

Numerical validation of a Eulerian hydrochemical code using a 1D multisolute mass transport system involving heterogeneous kinetically controlled reactions

F. Gérard *, A. Clément, B. Fritz

Centre de Géochimie de la Surface, CNRS (UPR 6251) 1, rue Blessig, Strasbourg 67084, France

Received 10 March 1996; revised 8 April 1997; accepted 29 April 1997

Abstract

It is demonstrated that at steady state, the 1D thermo-kinetic hydrochemical Eulerian mass balance equations in pure advective mode are indeed identical to the governing mass balance equations of a single reaction path (or geochemical) code in open system mode. Thus, both calculated reaction paths should be theoretically identical whatever the chemical complexity of the water–rock system (i.e., multicomponent, multireaction zones kinetically and equilibrium-controlled). We propose to use this property to numerically test the thermo-kinetic hydrochemical Eulerian codes and we employ it to verify the algorithm of the 1D finite difference code KIRMAT. Compared to the other methods to perform such numerical tests (i.e., comparisons with analytical, semi-analytical solutions, between two Eulerian hydrochemical codes), the advantage of this new method is the absence of constraints on the chemical complexity of the modelled water–rock systems. Moreover, the same thermo-kinetic databases and geochemical functions can be easily and mechanically used in both calculations, when the numerical reference comes from the Eulerian code with no transport terms (u and $D = 0$) and modify to be consistent with the definition of the open system mode in geochemical modelling. The ability of KIRMAT to treat multicomponent pure advective transport, subjected to several kinetically equilibrium-controlled dissolution and precipitation reactions, and to track their boundaries has been successfully verified with the property of interest. The required numerical validation of the reference calculations is bypassed in developing the Eulerian code from an already checked single reaction path code. A forward time-upstream weighting scheme (a mixing cell scheme) is used in this study. An

* Corresponding author. Earth Sciences Division, Lawrence Berkeley National Laboratory and Department of Geology and Geophysics, Earth Resources Center, University of California, Berkeley, CA 94720-4767, USA.

PII S0169-7722(97)00047-8

appropriate choice of grid spacing allows to calculate within the grid size uncertainty the correct mineral reaction zone boundaries, despite the presence of numerical dispersion. Its correction enables us to improve the convergence and to extend the numerical test to mixed advective–dispersive mass transport. However, the skewness factor involves numerical oscillations that prevent to compute different grid spacing. The use of a different chemically controlled time step constraint in both calculations induces some inconsistencies into the validation tests. This numerical validation method may be applied as well as to check a thermo-kinetic hydrochemical finite element based code, from a 1D heterogeneous systems, and 2D–3D systems provided that they are designed so as to be 1D equivalent. A one-step algorithm and the use of a numerical reference coming from the Eulerian code to be tested ensure the potential success (accuracy) of the numerical validation method.

1. Introduction

For many years, the development of mass transfer models in porous media has been of considerable interest to earth scientists, as they are needed to understand and quantify metamorphic alterations, mineral diagenesis and ore deposits and, ultimately, to predict migration of radionuclides and chemical contaminants. For this purpose, an increasing number of reactive transport (or hydrochemical) codes have been published (e.g., Novak, 1993; Steefel and Lichtner, 1994; Steefel and Lasaga, 1994). The most advanced may integrate 1D–2D advective and dispersive solute transport in saturated porous media, with aqueous speciation and gas equilibrium, subjected to full mechanistic kinetic rate laws for mineral precipitation and/or dissolution with possibilities for partial local equilibrium heterogeneous reactions. In their full form, the governing mass balance equations for multicomponent reactive solute transport are nonlinear and, therefore, must be solved with numerical methods, with a large advantage for Eulerian ones, where the reference frame is a rock volume (REV). These are easier to handle for complex systems than the Lagrangian (the reference frame is a moving fluid mass) and mixed Eulerian–Lagrangian methods (Fabriol et al., 1993).

Before any use of such sophisticated computer tools in application to practical studies, the numerical validation or verification of their algorithm must be successfully achieved. This is generally performed by comparing the numerical results to those obtained from an analytical or a semi-analytical solution of the mass transport equation. However, exact solutions only exist for very simple or idealized water–rock systems in comparison with the standard applications of the reactive transport modelling, especially when kinetic dissolution and precipitation processes are considered. A comprehensive review shows that they only exist for isothermal and homogeneous semi-infinite porous media, with steady flow and transport of one dissolved component subjected to a first-order kinetic rate law (Lichtner, 1988), or for pure diffusion (Lichtner et al., 1986; Lichtner, 1991) or pure advective transport (Walsh et al., 1984; Novak et al., 1988) of two or three reactive components handled by two equilibrium-controlled reactions. To perform some numerical tests in standard application conditions, it is possible to compare two equivalent Eulerian based hydrochemical codes. However, the reference model must be also numerically validated and above all both codes have to use the same geochemical functions (e.g., kinetic laws) and thermodynamic databases. This is particu-

larly difficult to achieve given the wide variety of databases used and the large differences existing among the chemical functions integrated (specially for kinetic rate laws).

The purpose of this paper is to propose and demonstrate a new method for performing the numerical verification stage for most of the thermo-kinetic hydrochemical codes whatever the chemical complexity of a 1D water–rock system. It is based on the steady state or stationary-state properties of the thermo-kinetic Eulerian reactive transport mass balance equations. Single reaction path (or geochemical) code calculations are used as numerical reference. Its great interest lies in the fact that such numerical reference is far easier tested numerically, given the lower complexity of the governing mass balance equations. In addition, the use of the tested Eulerian code with no transport terms as numerical reference naturally leads to use the same chemical functions and databases for both calculations to compare.

We investigate this property on the 1D finite difference reactive transport code KIRMAT (Gérard et al., 1996; Gérard, 1997). The first part of this paper is intended to present the theoretical basis of this study. A numerical validation test is performed and discussed during the second part. The third part is intended to discuss the applicability of this method to other codes and heterogeneous porous media.

2. Theory

2.1. Eulerian governing mass balance equations

The set of governing reactive transport mass balance equations is commonly based on the two following assumptions: all the aqueous species have the same diffusion coefficients and the rates of the homogeneous reactions are sufficiently faster than the other mass transfer processes so that the local equilibrium approximation (LEA) becomes valid. These approximations allow to reduce the number of independent variables from $N_{\text{tot.}}$ aqueous species to N_C primary species, one for each dissolved chemical element. According to these principles, the governing mass balance equations are usually expressed and solved in terms of total concentrations in primary species, or generalized concentrations. When reactive transport only involves dissolution and precipitation, both kinetic and equilibrium-controlled (LEA), one may write:

$$\frac{\partial}{\partial t}\left[\omega\psi_j + \sum_{k=1}^{N_k} \nu_{jk}(V_k)^{-1}\phi_k\right] + \nabla\cdot\left(u\psi_j - D\nabla\psi_j\right) = -\sum_{m=1}^{N_m} \nu_{jm}\frac{\partial \Xi_m}{\partial t} \tag{1}$$

Where ω stands for the flow porosity of the rock control volume, Ψ_j is the total concentration (in mole per water mass or volume) of the j primary aqueous species, N_k the set of mineral reacting reversibly, ν_{jk} the number of moles of species j in mineral k (equilibrium-controlled), V_k the molar volume of mineral k, and ϕ_k its volume fraction, u is the Darcy velocity (LT^{-1}), D the hydrodynamic dispersion tensor (L^2T^{-1}), Ξ_m denotes the reaction rate density, equivalent to the rate of precipitation or dissolution of mineral m per unit of the rock and fluid system, ν_{jm} is the number of moles of j in

mineral m, and N_m is the number of kinetic reactants in the rock (by convention, Ξ_m is taken as positive for precipitation and as negative for dissolution reactions).

The total concentration Ψ_j is given by:

$$\psi_j = C_j + \sum_{i=1}^{N_X} \nu_{ji} X_i \tag{2}$$

Where C_j is the concentration of primary species, X_i the concentration of secondary species i belonging to the set N_x $(=N_{\text{tot.}} - N_C)$, ν_{ji} is the molar stoichiometric coefficient of species j in secondary species i.

The reversible or equilibrium-controlled reactions provide an algebraic link between the primary and secondary species via the mass action law for each reaction. Each reversible homogeneous and heterogeneous reaction requires to solve a mass action equation.

2.2. *Eulerian steady state limit and single reaction path model governing mass balance equations*

The steady state limit of the set of equations in Eq. (1) is reached when the term involving the partial time derivative of the solute concentration is negligible compared to the remaining terms. The alteration of the host rock (i.e., mineral abundance, porosity, permeability, etc.) must occur sufficiently slowly compared to the time required to form a steady state, corresponding to a particular alteration stage of the porous media (Lichtner, 1988). For 1D systems, the governing mass balance Eq. (1) becomes:

$$u\frac{\partial \psi_j}{\partial x} - D\frac{\partial^2 \psi_j}{\partial x^2} = -\frac{\partial}{\partial t}\left[\sum_{k=1}^{N_k} \nu_{jk}(V_k)^{-1}\phi_k\right] - \sum_{m=1}^{N_m} \nu_{jm}\frac{\partial \Xi_m}{\partial t} \tag{3}$$

Geochemical or single reaction path computer codes are designed to calculate the speciation of aqueous solutions, the equilibrium state of a mineral assemblage and the time evolution of the system through a succession of states of partial equilibrium, successively affected by heterogeneous irreversible kinetic reactions. A single reaction path is calculated because the fluid composition evolves along a single path in composition space from its initial starting configuration to a final state of stable or metastable equilibrium (Lichtner et al., 1987). This forms a steady state. For dissolution and precipitation reactions, the corresponding governing mass balance equations may be expressed as:

$$\frac{\mathrm{d}\psi_j}{\mathrm{d}t} = -\frac{\mathrm{d}}{\mathrm{d}t}\left[\sum_{k=1}^{N_k} \nu_{jk}(V_k)^{-1}\phi'_k\right] - \sum_{m=1}^{N_m} \nu_{jm}\frac{\mathrm{d}\xi_m}{\mathrm{d}t} \tag{4}$$

Where ϕ'_k is the volume fraction of k minerals per units of fluid mass (usually 1 kg of water), ξ_m denotes the reaction rate density for a reaction path model, equivalent to the rate of precipitation or dissolution of mineral m per unit of fluid mass (taken as positive for precipitation and negative for dissolution).

Calculations could be done either in closed or open system with respect to the reacting minerals. The open system mode leads to a Lagrangian representation of pure advective reactive transport, because the reaction path may be interpreted as representing the effect of a single packet of moving fluid in contact with a set of reacting minerals. As the packet of fluid moves downstream, secondary minerals precipitating from the fluid are left behind and thus do not back-react with it.

The Lagrangian equation of fluid motion at the center of gravity of the fluid mass allows us to relate the fluid packet evolution in time with its space-travel along the flow path. In a homogeneous porous medium with constant flow rate, the propagation velocity of the fluid packet is given by:

$$\frac{\mathrm{d}x}{\mathrm{d}t} = \frac{u}{\omega} \tag{5}$$

Substituting the expression of $\mathrm{d}t$ from Eq. (5) into the left hand term of Eq. (4) and using the relation $\omega\phi'_k$ we obtain:

$$\frac{u}{\omega}\frac{\mathrm{d}\psi_j}{\mathrm{d}x} = -\frac{\mathrm{d}}{\mathrm{d}t}\left[\sum_{k=1}^{N_k} \nu_{jk}(V_k)^{-1}\phi'_k\right] - \sum_{m=1}^{N_m} \nu_{jm}\frac{\mathrm{d}\xi_m}{\mathrm{d}t} \tag{6}$$

This equation is strictly equivalent to Eq. (3) with $D = 0$. The single derivative nature of Eq. (6) is inherent to the Lagrangian formulation and may be converted to partial derivative (Eulerian formulation) using the classical Eq. (7). For the 1D mass transport function $\Psi_j = f(x, t)$, we obtain:

$$\mathrm{d}\psi_j = \left(\frac{\partial\psi_j}{\partial x}\right)_t \mathrm{d}x + \left(\frac{\partial\psi_j}{\partial t}\right)_x \mathrm{d}t \tag{7}$$

at steady state Eq. (7) reduces to:

$$\frac{\mathrm{d}\psi_j}{\mathrm{d}x} = \frac{\partial\psi_j}{\partial x} \tag{8}$$

It is mathematically demonstrated that the steady state limit of the Eulerian reactive transport mass equations (Eq. (3)) is strictly equivalent to the Lagrangian formulation applied to one packet of fluid (Eq. (6)) which may be calculated with a simple single reaction path geochemical code in open system mode. Thus, the same concentration profiles and the same reaction zone boundaries are expected in comparing the steady state results obtained with a Eulerian hydrochemical model to those calculated with a single reaction path or geochemical code in open system mode.

2.3. Numerical validation condition

A successful numerical validation of a Eulerian code with the property of interest may be theoretically expected if the modelled water–rock system is rigorously the same, the quasi-stationary state approximation is performed (i.e., all the transport, thermodynamic and kinetic parameters are kept constant during the Eulerian calculations), the Eulerian numerical method is capable of treating pure advective mass transport (i.e.,

without the appearance of numerical instabilities), and the thermodynamic databases or parameters used in both codes are the same. Note that no constraints exist on the initial solute concentration required in a Eulerian hydrochemical model, given that with the Lagrangian formulation in pure advective mode the initial fluid is flushed out of the column by the first fluid packet (Lichtner, 1992).

Typically the greatest difficulty for Eulerian methods in solving the solute transport partial differential equation (PDE) arises when advective transport is dominant. This may result in nonphysical oscillations in the vicinity of sharp concentration fronts, depending on the finite difference (or FD) formulation used for the first spatial derivative appearing in the advective term. Modelling pure advective mass transport is stable with an FD scheme corresponding to the well known mixing cell models (see review of Bajracharya and Barry, 1993). These are the explicit–backward or forward time-upstream weighting formulation (Van Ommen, 1985), the implicit–backward or backward time-upstream weighting differencing (Dudley et al., 1991) and a mixed explicit–implicit backward formulation (Bajracharya and Barry, 1993).

The last validation condition may be easily achieved by using the tested hydrochemical code with no transport terms ($u = 0$ and $D = 0$), appropriately modified to be consistent to the open system mode. This numerical reference can be numerically checked from various multicomponent systems subjected to one kinetic (n-order) and several equilibrium-controlled heterogeneous reactions by using a simple commercial spreadsheet program (Steinmann et al., 1994) or manual calculations as references. Alternatively, the hydrochemical model to be checked could come from an already tested geochemical code where transport is added to the chemical mass balance equations as a sink/source term. This method has been used to develop the code KIRMAT to be tested.

3. Model description

The Eulerian thermo-kinetic hydrochemical code KIRMAT (Gérard et al., 1996; Gérard, 1997) has been developed from the single reaction path model KINDIS (Madé et al., 1994), by keeping all its geochemical formulation and its numerical method to solve chemical equations.

The thermo-kinetic geochemical code KINDIS was developed from the purely thermodynamic code DISSOL (Fritz, 1975; Fritz and Tardy, 1976), which in turn originated from PATH1 (Helgeson et al., 1970). Theoretical kinetic rate laws for mineral dissolution and precipitation based on the Transition State Theory (TST) have been implemented in DISSOL. These geochemical codes have been intensively numerically tested and used in published studies on hydrothermal, diagenetic and weathering processes (e.g., Noack et al., 1993; Bertrand et al., 1994).

In KINDIS, the irreversible kinetic driving force is explicitly calculated and the sequence of partial equilibrium state is calculated from second-order Taylor series expansions.

In KIRMAT, solute transport is added to kinetic dissolution and/or precipitation reactions. A chemically controlled time step (noted Δt_c) allows to preserve accuracy of the calculations. Its value is chosen inversely proportional to the largest of the first

derivative variations among all the solute concentrations, and is controlled by setting the θ parameter (inversely proportional to Δt_c). The set of PDEs is integrated along one direction with the classical finite difference approximation method. An explicit scheme and a one-step algorithm are used to solve simultaneously the chemical (from KINDIS) and the conservative transport mass balance equations. A classical mixing cell scheme, the explicit–backward discretization, is computed for a numerical validation study with the property of interest. It involves less numerical dispersion than the other mixing cell scheme (Bajracharya and Barry, 1993).

The second-order truncation error, or numerical dispersion, may be removed by subtracting its predicted value from the FD physical dispersive flux expression (e.g., de Marsily, 1986). This correction improves the numerical results and thus enables us to achieve closer comparisons with the proposed numerical reference. However, the explicit finite difference scheme requires the maximum time step to be limited by the convergence criteria (Eq. (9)), while pure advective transport needs to respect the less constraining Courant criterion (e.g., de Marsily, 1986).

$$\Delta t_{D_{\text{num.}}} \leq \frac{\lambda \Delta x^2}{D_{\text{num.}}} \tag{9}$$

Where $D_{\text{num.}}$ stands for the numerical dispersion and λ is a constant (must be ≤ 0.5).

4. Numerical tests

From a theoretical point of view, any 1D water–rock systems may be modelled to test the hydrochemical code KIRMAT with the property of interest. Darcy velocity, flow porosity, and reactive surface area of the whole rock do not modify the reaction path. They only shift the absolute positions of the reaction zone boundaries with the same scaling factor (see Lichtner, 1993). However, kinetic parameters (reactive surfaces, apparent rate constants) must be optimized in order to individually track mineral reaction zone boundaries with a modest number of equally spaced grid points. This requirement comes from the presence of numerical oscillations arising when the backward–explicit scheme is computed and the numerical dispersion is removed with different grid spacing. This numerical artifact or skewness factor, due to third-order spatial truncation errors, alters the concentration profiles and no general criteria or correction terms are available at present for avoiding it (Moldrup et al., 1994).

4.1. Numerical reference: Lagrangian calculations

By solving Eq. (4), the numerical reference (KINDIS) deals with a fractured homogeneous granite at ambient temperature (25°C) subjected to pure advective infiltration of a hyperalkaline solution. Ferrous biotite is present to test the redox system. The ratio $u{:}\omega$ is assumed equal to 10 m/yr and comparisons are accordingly done on the first 2 m of the rock column which theoretically includes four mineral reaction zone boundaries (Table 1).

Table 1
Numerical reference: positions in time and space ($u/\omega = 10$ m/yr) of the mineral reaction zone boundaries calculated with the single reaction path code KINDIS in open system mode

Mineralogical events	Reaction formulation	Fluid packet travel time t (yr)	Percolation distance x (m)
Goethite precipitation	Equilibrium-controlled	1×10^{-17}	1×10^{-16}
Laumontite precipitation	Kinetically controlled	8.086×10^{-2}	0.8086
Analcime precipitation	Kinetically controlled	1.0764×10^{-1}	1.0764
K-feldspar saturation	Kinetically controlled	1.7648×10^{-1}	1.7648
Column outlet		0.2	2

4.2. *Pure advective mode comparisons*

The 2-m column is discretized into 10, 50, and 250 equally spaced grid blocks of 0.2, 0.04 and 0.008 m length, respectively. The code KIRMAT solves Eq. (3) without the dispersive term. Figs. 1 and 2 illustrate the satisfactory results obtained in comparing KIRMAT steady state pH and Eh profiles, for example, with the numerical reference results. Convergence or truncature errors decrease consistently with grid spacing. Steady state pH and redox potential Eh are slightly larger and smaller, respectively. This is consistent with the presence of the well-known back or reverse dispersion artifact. The sigmoidal convergence error trend on pH illustrated in Fig. 3 stems from the pH spatial gradient amplitude.

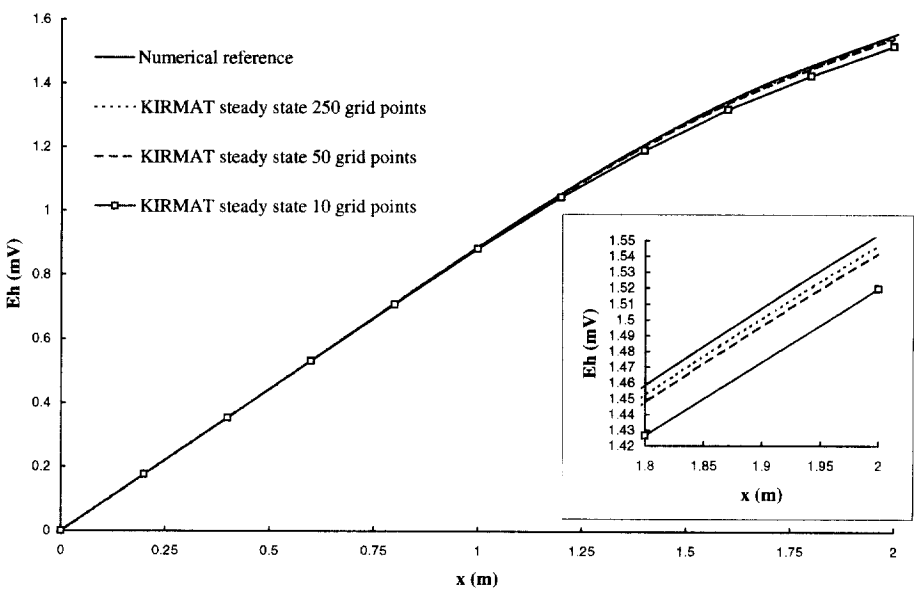

Fig. 1. Comparison between the numerical reference and KIRMAT at steady state for Eh spatial variations when decreasing grid spacing Δx. A complete convergence of the finite difference approximation might be consistently obtained for $\Delta x \rightarrow 0$.

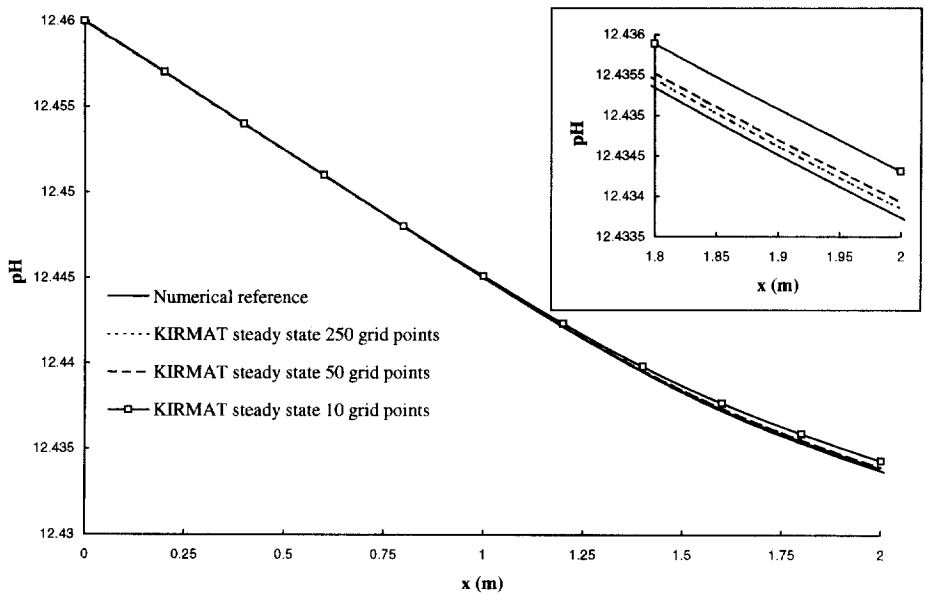

Fig. 2. Comparison between the numerical reference and pH steady state profiles when decreasing grid spacing. The steady state pH variations are always higher than the numerical reference. This comes from the back-dispersion effect for reverse solute parameter gradients.

The steady state positions of the four reaction zone boundaries are compiled in Table 2. Although, within the grid spacing uncertainty, goethite, laumontite and analcime reaction zone boundaries are always correctly positioned at steady state, the K-feldspar

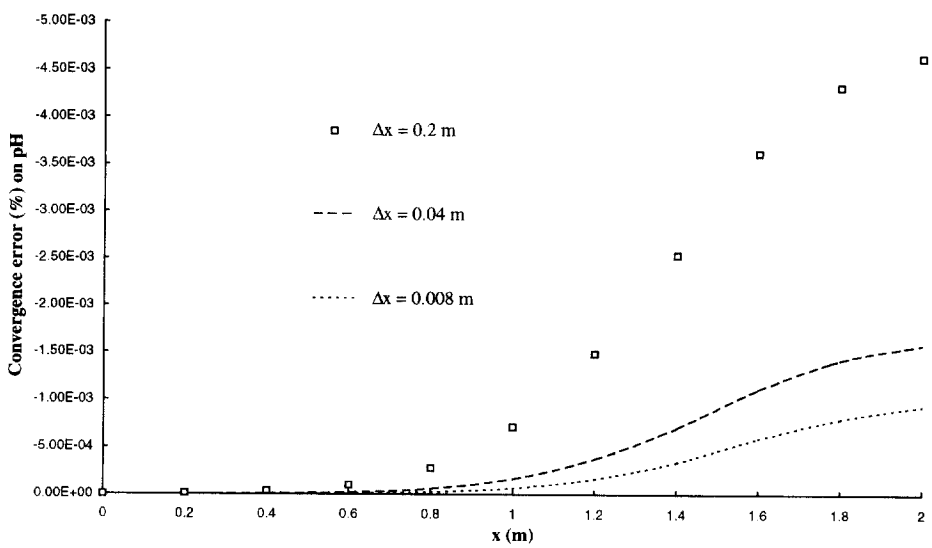

Fig. 3. Convergence error on pH (percentage). The sigmoidal trend is linked to the pH spatial gradient evolution.

Table 2
Positions of the mineral reaction zone boundaries calculated at steady state with KIRMAT in pure advective mode. Italic typed distances are corresponding to delayed positions of the reaction zones within the control volume uncertainty

Mineralogical events	Numerical reference (m)	KIRMAT $\Delta x = 0.2$ m uncertainty ± 0.1 m	KIRMAT $\Delta x = 0.04$ m uncertainty ± 0.02 m	KIRMAT $\Delta x = 0.008$ m uncertainty ± 0.004 m
Goethite precipitation	1×10^{-16}	0.1	0.02	0.004
Laumontite precipitation	0.8086	0.9	0.82	0.812
Analcime precipitation	1.0764	1.1	1.06	1.076
K-feldspar saturation	1.7648	*1.9*	1.78	*1.772*

saturation limit is slightly delayed toward downstream for 0.2 and 0.008 m grid spacing. This is consistent with the larger convergence error (Figs. 1–3), acting in this example to lower the spatial variations of the K-feldspar ionic activity product. However, for $\Delta x = 0.04$ m (50 grid points), the K-feldspar saturation boundary is positioned well within the grid size uncertainty (± 0.02 m), while the numerical dispersion is more important than with $\Delta x = 0.008$ m grid spacing.

This surprising and apparently conflicting result comes from the theoretical position of this reaction boundary between two consecutive grid points. When the K-feldspar reaction zone boundary should theoretically appear near to the upstream limit of a control volume, the numerical dispersion effects may be too low to shift it out from the latter. Such distances for the K-feldspar saturation boundary are reported in Table 3. They are obviously grid size-dependent. With slightly finer grid spacing ($\Delta x = 0.039$ m), inferring a slightly lower truncation error, the theoretical K-feldspar saturation boundary position inside the control volume is closer to the next downstream one. Modelling results for $\Delta x = 0.039$ m are consistent with the above discussion: the steady state K-feldspar saturation boundary is effectively delayed toward downstream (saturation at 1.8135 ± 0.0195 m).

Table 3
Relative position (percentage) of K-feldspar saturation boundary at steady state within the predicted or theoretical control volume, calculated from the numerical reference results (see Table 1). With $\Delta x = 0.039$ m, involving a slightly weaker convergence error in comparison to $\Delta x = 0.04$ m, due to the numerical dispersion effect the relative position of K-feldspar saturation boundary is closer from the next downstream control volume, where this reaction front is expected to occur at steady state

Grid size Δx (m)	Corresponding grid point number to complete the 2-m profile length	Relative position within the redicted control volume (%)
0.2	10	82.4
0.04	50	12
0.039	*51.28*	*25.1*
0.008	250	60

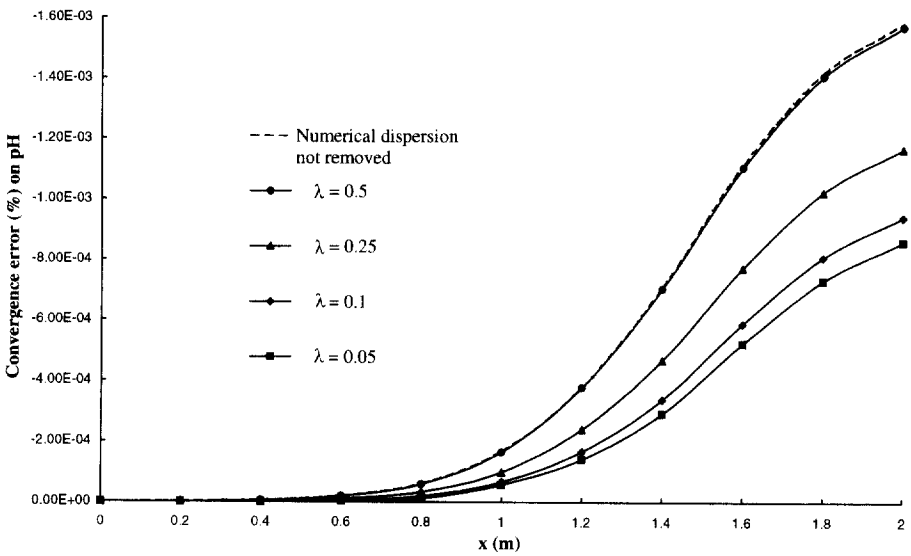

Fig. 4. Convergence error on pH (%) for $\Delta x = 0.2$ m and numerical dispersion removed. At a given grid size Δx, the local discretization error depends on the value imposed for the dispersive convergence criteria λ (Eq. (9)).

4.3. Numerical dispersion corrected

The ability of KIRMAT to accurately track multireaction zone boundaries has been confirmed with the above calculations, with a minor discrepancy for the K-feldspar saturation boundary. A better convergence is expected when the numerical dispersion is removed. Furthermore, such a correction would also enable us to numerically test the ability of the KIRMAT algorithm to model the dispersive transport. The correction method proposed by Lantz (1971) is used. Eq. (3) is then solved with $D = -D_{num}$.

The decrease of the λ value (Eq. (9)) produces an increasing convergence of the code KIRMAT (Fig. 4). A similar convergence error trend is consistently observed in decreasing the grid size at a given λ value. An accurate position for the K-feldspar saturation boundary is calculated with $\Delta x = 0.2$ when $\lambda \leq 1/4$, while the λ value had to be far lower ($\lambda < 1/20$) with $\Delta x = 0.008$ m. This result also stems from the lower grid size uncertainty (± 0.004 m).

4.4. Chemically controlled time step values sensitivity

Fig. 5 illustrates the pH variations used as numerical reference over a local part of the 2-m profile length (for clarity) calculated with lower and higher θ values (Section 3) than it was previously done. This comes from the numerical approximation (i.e., second-order Taylor expansion series) required for both calculations (i.e., reference and KIRMAT), converging toward the exact solution of this reactive transport problem when $\Delta t_c \rightarrow 0$, attained for $\theta \rightarrow \infty$. The convergence error trends are altered (Fig. 6) when

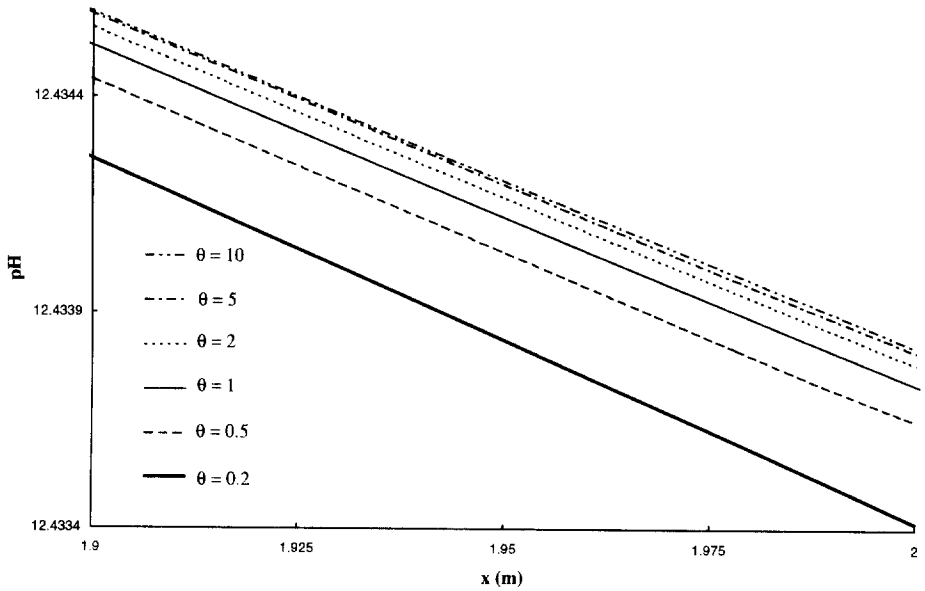

Fig. 5. pH profiles calculated with KINDIS in open system (Lagrangian representation) with different θ values (Section 3). For $\theta \rightarrow \infty$ (i.e., $\Delta t_c \rightarrow 0$), the Lagrangian calculations tend towards the exact solution.

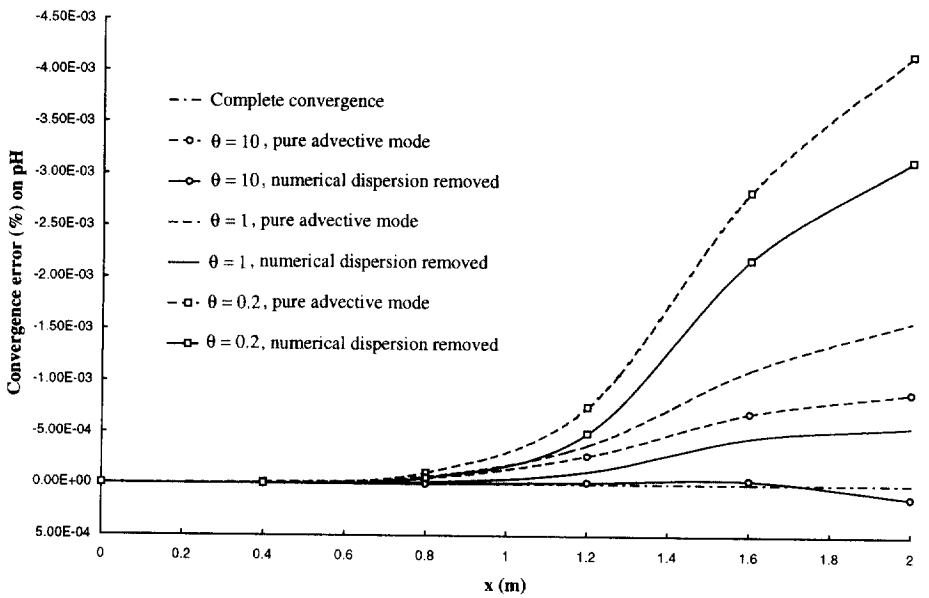

Fig. 6. Convergence error on pH (%), obtained in comparing the KIRMAT steady state results for θ (Section 3) with three slightly different numerical references calculated with KINDIS in open system mode for $\theta = 0.2$ (square), $\theta = 1$ (no symbol) and $\theta = 10$ (circle). Dashed line in pure advective mode, continuous line when numerical dispersion is removed. A higher θ-value artificially improves the results.

using a different θ value to calculate the numerical reference than for KIRMAT calculations. In this example, a comparison of the 0.2θ-numerical reference with the θ-related (lower Δt_c) steady state result shows an exceedingly higher convergence error. With a lower Δt_c for the numerical reference, the reverse trend is observed. The result becomes inconsistent for 10θ, by exhibiting an artificially normal convergence value for reversed solute parameter gradients. This effect disappears in setting the same constraint on Δt_c for both calculations.

5. Discussion

The present Eulerian and Lagrangian mass balance equations only involve mixed kinetic–equilibrium dissolution and precipitation reactions. However, this new approach for numerical validation of thermo-kinetic Eulerian hydrochemical codes may be used as well with any heterogeneous reactions (e.g., adsorption–desorption), provided that a steady state representation is also performed for these phenomena. Furthermore, although the numerical validation tests in this paper addressed only isothermal and homogeneous porous media, this new validation method might also be performed for 1D heterogeneous porous media with steady temperature variations. Then, the numerical reference should be obtained from successive single reaction path calculations; one model run will be required for each homogeneous and isothermal part of the total profile or column, and the outlet composition of the fluid packet must be used as inlet composition in the next downstream column part. In addition, 2D and 3D Eulerian calculation could also be tested with the method of interest. For example, to verify such a code along the x-axis, it is necessary to reduce the 2D or 3D system to an equivalent 1D one (i.e., homogeneous water–rock system in the other directions, in term of mass, heat transport and chemical parameters, etc. and boundary conditions).

A finite element technique with upstream-weighting may also be used to compute pure advective transport (de Marsily, 1986 and reference therein). Thus, this new approach is not limited to mixing cell scheme and the FD method. In addition, some upstream weighting higher order schemes may also model pure advective transport (see review of Chen and Falconer, 1994). They are free of numerical dispersion and, as a consequence, different grid spacing may be used (i.e., no numerical dispersion correction is needed, thus, no skewness factor) to carry out the numerical test of an Eulerian thermo-kinetic hydrochemical code with the steady state property investigated in this paper. However, such schemes cannot be used to test advective and dispersive reactive transport regime with the method of interest, when numerical dispersion is corrected. Taylor series analysis and numerical tests remain to be done for other mixing cell schemes, which are associated with larger second-order truncation error.

We have emphasized before (Figs. 5 and 6) that the use in both calculations (i.e., Lagrangian and Eulerian) of a different chemically controlled time step (Δt_c) in response to the same driving force may entail some inconsistent numerical validation results. Thus, a better agreement is expected if these numerical tests are performed using in both codes the same solution method for the set of nonlinear equations, and the same constraint on the Δt_c value. Moreover, given that explicit formulations decouple the

chemical kinetic term from the reversible one (Lichtner, 1985), a numerical check of a Eulerian hydrochemical code with an implicit solution method against an explicit single reaction path code (like KINDIS) is necessary limited. Thus, a more confident numerical validation is expected with a one-step algorithm, and a numerical reference calculated from the Eulerian code in open system mode with no transport (u and $D = 0$).

Finally, the presence of an inherent mass balance error when using an operator-splitting or a two-step algorithm for problems involving a continuous mass influx boundary (Valocchi and Malmstead, 1992) also requires to use a one-step algorithm for accurate comparisons, whatever the origin of the numerical reference (i.e., the present method or an analytical or semi-analytical solution). Because mass balance errors increase with increasing product $k \cdot \Delta t$ (where k is a rate constant), this limitation must be more sensitive when reversible heterogeneous reactions are considered.

6. Conclusion

The validation tests in this paper show a good agreement between the single reaction path calculations (KINDIS) and the finite difference (FD) code KIRMAT at steady state. The capacity to model either 1D pure advective or advective–dispersive (numerical correction induced) reactive multicomponent transport, and to track homogeneous/heterogeneous multireaction zone boundaries, has been checked. This new numerical validation method may even be theoretically applied to 1D heterogeneous porous media, and to 2D–3D systems provided that they lead to an equivalent 1D profile. Mixing cell FD formulations and the finite element upstream-weighting function involve more or less numerical dispersion. Nonetheless, appropriate choice of the grid size makes it possible to obtain the correct mineral reaction zone boundaries at steady state. In addition, the numerical dispersion artifact is in turn an advantage because its correction allows to extend the application range of this new method to multicomponent advective and numerical dispersive solute transport. However, using an explicit–backward scheme, numerical oscillations arise when applying numerical dispersion corrections in non-uniform grids. This probably third-order numerical artifact requires to use appropriate kinetic parameters in order to individually track several reaction zones without an excessive number of equally spaced grid blocks. Some more accurate higher order FD schemes allow to make calculations with different grid sizes in a pure advective mode. However, they are free of numerical dispersion and prevent numerical test of advective–dispersive regimes given no numerical dispersion need to be removed. The use of a numerical reference calculated from the Eulerian code to be tested without transport term and a one-step algorithm would preserve the potential success of the numerical validation stage. The test of the numerical accuracy of the geochemical calculations may be carried out for rather sophisticated water–rock systems (hence, one of the interest of the proposed numerical validation method for hydrochemical codes), by using preexisting, already numerically checked, thermo-kinetic geochemical codes.

Given the numerous advantages of this new method to perform the numerical validation stage of hydrochemical thermo-kinetic codes in regard to the alternative approach in which two Eulerian codes are compared, it will be very useful for developers of reactive chemical migration models in porous media.

Acknowledgements

The authors acknowledge the financial support of the Centre National de la Recherche Scientifique and of the Société de Secours des Amis des Sciences. We are grateful to K. Pruess (Lawrence Berkeley National Laboratory) for his thoughtful correction of the English language.

References

Bajracharya, K., Barry, D.A., 1993. Mixing cell models for nonlinear equilibrium single species adsorption and transport. J. Contam. Hydrol. 12, 227–243.

Bertrand, C., Fritz, B., Sureau, J.-F., 1994. Hydrothermal experiments and thermo-kinetic modelling of water–sandstone interactions. Chem. Geol. 116, 189–202.

Chen, Y., Falconer, R.A., 1994. Modified forms of the third-order convection, second-order diffusion scheme for the advection–diffusion equation. Adv. Water Res. 17, 147–170.

Dudley, L.M., Mclean, J.E., Furst, T.H., Jurinak, J.J., 1991. Sorption of cadmium and copper from an acid mine waste extract by two calcareous soils: column studies. Soil Sci. 151, 121–135.

Fabriol, R., Sauty, J.P., Ouzounian, G., 1993. Coupling geochemistry with a particle tracking transport model. J. Contam. Hydrol. 13, 117–129.

Fritz, B., 1975. Etude thermodynamique et simulation des réactions entre minéraux et solutions. Application à la géochimie des altérations et des eaux continentales. Sci. Géol. Mém. 41, 152.

Fritz, B., Tardy, Y., 1976. Séquences des minéraux secondaires dans l'altération des granites et roches basiques; modèles thermodynamiques. Bull. Soc. Géol. France 18, 7–12.

Gérard, F., 1997. Modélisation géochimique thermodynamique et cinétique avec prise en compte des phénomènes de transport de masse en milieu poreux saturé. Thèse Univ. Louis Pasteur, Strasbourg, 250 pp.

Gérard, F., Clément, A., Fritz, B., Crovisier, J.-L., 1996. Introduction des phénomènes de transport dans le modèle thermo-cinétique KINDIS: Le modèle KIRMAT. C.R. Acad. Sci. Paris 322 (IIa), 377–384.

Helgeson, H.C., Brown, T.H., Nigrini, A., Jones, T.A., 1970. Calculations of mass transfer in geochemical processes involving aqueous solutions. Geochim. Cosmochim. Acta 34, 569–592.

Lantz, J., 1971. Quantitative evaluation of numerical diffusion (truncation error). Soc. Pet. Eng. 11, 315–320.

Lichtner, P.C., 1985. Continuum model for simultaneous chemical reactions and mass transport in hydrothermal systems. Geochim. Cosmochim. Acta 49, 143–165.

Lichtner, P.C., 1988. The quasi-stationary state approximation to coupled mass transport and fluid–rock interaction in a porous media. Geochim. Cosmochim. Acta 52, 143–165.

Lichtner, P.C., 1991. The quasi-stationary state approximation to fluid–rock reactions: local equilibrium revisited. in: Ganguly, J. (Ed.), Diffusion, Atomic Ordering and Mass Transport. Adv. Phys. Geochem. 8, 454-562.

Lichtner, P.C., 1992. Time–space continuum description of fluid–rock interaction in permeable media. Water Resour. Res. 28, 3135–3155.

Lichtner, P.C., 1993. Scaling properties of time–space kinetic mass transport equations and the local equilibrium limit. Am. J. Sci. 293, 257–296.

Lichtner, P.C., Oelkers, E.H., Helgeson, H.C., 1986. Exact and numerical solutions to the moving boundary problem resulting from reversible heterogeneous reactions and aqueous diffusion in a porous media. J. Geophys. Res. 91, 7531–7544.

Lichtner, P.C., Helgeson, H.C., Murphy, W.M., 1987. Lagrangian and Eulerian representations of metasomatic alteration of minerals. in: Helgeson, H.C. (Ed.), Chemical Transport in Metasomatic Processes. Reidel, 519–545.

Madé, B., Clément, A., Fritz, B., 1994. Modelling mineral/solution interactions: the thermodynamic and kinetic code KINDISP. Comput. Geosci. 20, 1347–1363.

de Marsily, G., 1986. Quantitative Hydrogeology. Academic Press, New York, 440 pp.

Moldrup, P., Yamaguchi, T., Rolston, D.E., Vestergaard, K., Hansen, J.Aa., 1994. Removing numerically induced dispersion from finite difference models for solute and water transport in unsaturated soils. Soil Sci. 157, 153–161.

Noack, Y., Colin, F., Nahon, D., Delvigne, J., Michaux, L., 1993. Secondary-mineral formation during natural weathering of pyroxene: review and thermodynamic approach. Am. J. Sci. 293, 111–134.

Novak, C.F., 1993. Modelling mineral dissolution and precipitation in dual-porosity fracture–matrix systems. J. Contam. Hydrol. 13, 91–115.

Novak, C.F., Schechter, R.S., Lake, L.W., 1988. Rule-based mineral sequences in geochemical flow processes. Am. Inst. Chem. Eng. J. 34, 1607–1614.

Steefel, C.I., Lasaga, A.C., 1994. A coupled model for transport of multiple chemical species and kinetic precipitation/dissolution reactions with applications to reactive flow in single phase hydrothermal systems. Am. J. Sci. 294, 593–620.

Steefel, C.I., Lichtner, P.C., 1994. Diffusion and reaction in rock matrix bordering a hyperalkaline fluid-filled fracture. Geochim. Cosmochim. Acta 58, 3595–3612.

Steinmann, P., Lichtner, P.C., Shotyk, W., 1994. Reaction path approach to mineral weathering reactions. Clays Clay Miner. 42, 197–206.

Valocchi, A.J., Malmstead, M., 1992. Accuracy of operator splitting for advection–dispersion reaction problems. Water Resour. Res. 28, 1471–1476.

Van Ommen, H.-C., 1985. The mixing-cell concept applied to transport of non-reactive and reactive components in soils and groundwater. J. Hydrol. 78, 201–213.

Walsh, M.P., Bryant, S.L., Schechtner, R.S., Lake, L.W., 1984. Precipitation and dissolution of solids attending flow through porous media. Am. Inst. Chem. Eng. J. 30, 317–328.